Identification of Stiffness and Damping via SPHS Excitation and Multi-DOF Active Magnetic Bearing-Rotor Model

Jiang KeJian[a, b]   Zhu ChangSheng[b]

a. College of Informatics and Electronics, Zhejiang Sci-Tech University, Hangzhou, China, 310016.
b. College of Electrical Engineering, Zhejiang University, Hangzhou, China, 310027.

***Abstract*: The equivalent stiffness and the equivalent damping are the important and commonly used parameters for representing the support characteristic of the Active Magnetic Bearing(AMB). A method for measuring the equivalent stiffness and the equivalent damping is proposed with parameter identification via the multi-frequency excitation. The parameter identification is based on the multi-degree of freedom(DOF) rotor model, not the single DOF model, which can not be suitably applied to the multi-DOF AMB-rotor system. Additionally, the Schroeder Phased Harmonic Sequences(SPHS) are applied to generate the signal for the multi-frequency excitation. SPHS can achieve the lowest peak value by means of appropriate selection for the relative phasing of each frequency component, so that the possibility of the rotor vibration exceeding clearances of AMB and the magnetic force reaching saturation is minimized. Finally, the experiments indicate that the proposed method can efficiently reduce the peak value for the superimposed multi-frequency excitation and correctly identify the equivalent stiffness and equivalent damping of the AMB-rotor system.**

***Keywords*: active magnetic bearing, multi-frequency excitation, Schroeder phased harmonic sequences, equivalent stiffness, equivalent damping**

1. Introduction

The active magnetic bearing(AMB) can not only provide the levitating support for the rotor without any mechanical friction, but also apply the real-time magnetic force to suppress the rotor vibration. For the performance advantages of the AMB technology, more and more attentions have been focused on the AMB application.

For either the traditional mechanical bearing or the active magnetic bearing, the support characteristic is the foundation for the rotor dynamics analysis. In the traditional mechanical bearing, the commonly used parametric representation for the support characteristic are the stiffness and the damping, which are also used for the active magnetic bearing, namely, the equivalent stiffness and the equivalent damping.

In recent years, there have been a great number of investigations into measuring and analyzing the AMB support characteristic. Tsai et al.[1] applied the wavelet transform algorithm to identify the magnetic damping and magnetic stiffness coefficients of the AMB system and analyzed their nonlinear order. Lim et al.[2] identified the equivalent stiffness and the equivalent damping for the AMB with the PID control strategy and analyzed the change rule of the support characteristic under the different PID parameters. Kim et al.[3] achieved to measure the force-current factor and the force-displacement factor by converging of adaptive filter. Mehmet et al.[4] and Lim et al.[5] presented the stiffness identification with multi-frequency excitation, which adopted the SPHS to avoid the superimposing peak of multi-frequency component. Bauomy et al.[6] investigated the response of the AMB-rotor system subjecting to a periodically time-varying stiffness. The stability of system near the simultaneous combined and sub-harmonic resonance was analyzed by the 4th Rung Kutta method. Sayyad et al. [7] presented the use of a variable stiffness type magnetic vibration absorber to control the vibration of a beam structure. Its principle is similar to the rotor vibration of AMB with variable stiffness in single DOF. Baloh et al. [8] proposed a method to measure the force-current factor and the force-displacement factor of AMB by adaptive estimation with least square algorithm.

2. Problem Formulation

In this study, the attention would be confined to solve two problems for measuring the stiffness and the

damping of the AMB-rotor system.

1: Most aforementioned methods proposed for measuring the stiffness and the damping of AMB are based on the levitation model in single degree of freedom(DOF), which can not be suitably applied to the multi-DOF rotor systems. A multi-DOF modeled parameter identification method is needed.

2: The multi-frequency excitation is a normal method for the parameter identification in AMB. It is desirable that each frequency component of the multi-frequency excitation should be strong enough so that the vibration responses of every component are vivid. However, the vibration peak due to superimposing all the frequency component may result in unacceptably large rotor vibration or cause force saturating of the AMB.

In this paper, a multi-DOF rotor model based method is proposed for measuring the stiffness and the damping via multi-frequency excitation. Schroeder Phased Harmonic Sequences(SPHS) is adopted to achieve the lowest peak value of the multi-frequency excitation by means of appropriate selection for the relative phasing of each components, so that the possibility of the vibration displacement exceeding clearances or the bearing force reaching saturation is minimized.

3. Identification of Stiffness and Damping with Multi-DOF Rotor model

If the AMB control system adopts the decentralized control for each DOF, namely, the AMB s control current in a certain direction is decided only by the rotor displacement in its own direction, the AMB support can be equivalent to two mutually perpendicular spring-damping structures as shown in Fig.1, which is the so-called equivalent stiffness and equivalent damping. It is similar to the concept of the traditional mechanical bearing.

Hereby, provided a rotor is supported by two AMBs, A and B, shown in Fig.1. The support of two AMBs are equivalent to 4 spring-damping structures in 4 directions respectively. The equivalent stiffness or the equivalent damping in a certain direction is decided only by the rotor displacement in its own direction respectively, namely, the spring-damping structures of every direction are independent each other.

In Fig.1, O is the mass center of the rotor, the distance between the rotor mass center and two AMBs respectively are l_a and l_b. The axis z is the rotating axis of the rotor.
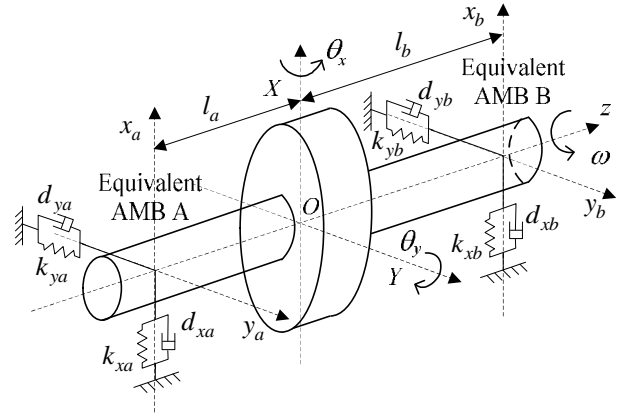

Fig.1 equivalent model forAMB-rotor system

The rotor attitude vector can be defined as $[X, q_y, Y, q_x]^T$, where, X, Y are the displacements of the rotor mass center in x and y directions, q_y and q_x are the angular displacements of rotor rotating around axis y and axis x. The positive directions of every motion are shown in Fig. 1.

Otherwise, the rotor attitude vector also can be defined by the rotor location in the place of two AMBs as $[x_a, x_b, y_a, y_b]^T$, where, x_a, y_a is the rotor's location coordinates in the place of the AMB A, and x_b, y_b is that of AMB B, as shows in Fig.1.

The transfer relation between two types of the rotor attitude vectors can be given as follows

$$\begin{bmatrix} X \\ q_y \\ Y \\ q_x \end{bmatrix} = \frac{1}{l}\begin{bmatrix} l_b & l_a & 0 & 0 \\ 1 & -1 & 0 & 0 \\ 0 & 0 & l_b & l_a \\ 0 & 0 & 1 & -1 \end{bmatrix}\begin{bmatrix} x_a \\ x_b \\ y_a \\ y_b \end{bmatrix} \quad (1)$$

Firstly, the equations of rotor motion can be written in the form of stiffness and damping, (In this paper, only the radial supports of rotor are considered and the gyroscopic effect is neglectable)

$$m\ddot{X} = -(d_{xa}\dot{x}_a + k_{xa}x_a) - (d_{xb}\dot{x}_b + k_{xb}x_b) + F_x$$
$$J\ddot{q}_y = -(d_{xa}\dot{x}_a + k_{xa}x_a)l_a + (d_{xb}\dot{x}_b + k_{xb}x_b)l_b + M_x \quad (2)$$
$$m\ddot{Y} = -(d_{ya}\dot{y}_a + k_{ya}y_a) - (d_{yb}\dot{y}_b + k_{yb}y_b) + F_y$$
$$J\ddot{q}_x = -(d_{ya}\dot{y}_a + k_{ya}y_a)l_a + (d_{yb}\dot{y}_b + k_{yb}y_b)l_b + M_y$$

Where, m is the mass of rotor, J is the transverse moment of inertia. F_x, F_y are the exciting forces respectively in direction x and y, and M_x, M_y are the exciting moments around the x axis and y axis respectively. The equivalent stiffness of every directions are denoted respectively by $k_{xa}, k_{xb}, k_{ya}, k_{yb}$, and that for the equivalent damping are $d_{xa}, d_{xb}, d_{ya}, d_{yb}$.

Eq.(2) is rebuilt by substitution of Eq.(1). The

following matrix equations can be obtained

$$\frac{1}{l}\begin{bmatrix} ml_b & ml_a & 0 & 0 \\ J & -J & 0 & 0 \\ 0 & 0 & ml_b & ml_a \\ 0 & 0 & J & -J \end{bmatrix}\begin{bmatrix} \ddot{x}_a \\ \ddot{x}_b \\ \ddot{y}_a \\ \ddot{y}_b \end{bmatrix} + \begin{bmatrix} d_{xa} & d_{xb} & 0 & 0 \\ d_{xa}l_a & -d_{xb}l_b & 0 & 0 \\ 0 & 0 & d_{ya} & d_{yb} \\ 0 & 0 & d_{ya}l_a & -d_{yb}l_b \end{bmatrix}\begin{bmatrix} \dot{x}_a \\ \dot{x}_b \\ \dot{y}_a \\ \dot{y}_b \end{bmatrix}$$

$$+ \begin{bmatrix} k_{xa} & k_{xb} & 0 & 0 \\ k_{xa}l_a & -k_{xb}l_b & 0 & 0 \\ 0 & 0 & k_{ya} & k_{yb} \\ 0 & 0 & k_{ya}l_a & -k_{yb}l_b \end{bmatrix}\begin{bmatrix} x_a \\ x_b \\ y_a \\ y_b \end{bmatrix} = \begin{bmatrix} F_x \\ M_x \\ F_y \\ M_y \end{bmatrix} \quad (3)$$

By the Laplace transform, the frequency domain equations of Eq.(3) is

$$\begin{bmatrix} -mw^2\frac{l_b}{l}+k_{xa}+jwd_{xa} & -mw^2\frac{l_a}{l}+k_{xb}+jwd_{xb} & 0 & 0 \\ -J\frac{w^2}{l}+k_{xa}l_a+jwd_{xa}l_a & J\frac{w^2}{l}-k_{xb}l_b-jwd_{xb}l_b & 0 & 0 \\ 0 & 0 & -mw^2\frac{l_b}{l}+k_{ya}+jwd_{ya} & -mw^2\frac{l_a}{l}+k_{yb}+jwd_{yb} \\ 0 & 0 & -J\frac{w^2}{l}+k_{ya}l_a+jwd_{ya}l_a & J\frac{w^2}{l}-k_{yb}l_b-jwd_{yb}l_b \end{bmatrix}$$

$$= \begin{bmatrix} F_x(jw) \\ M_x(jw) \\ F_y(jw) \\ M_y(jw) \end{bmatrix}\begin{bmatrix} x_a(jw) \\ x_b(jw) \\ y_a(jw) \\ y_b(jw) \end{bmatrix}^{-1}$$

(4)

To simplify the expression, let

$$\begin{aligned} A_{xa} &= k_{xa} + jwd_{xa} \\ A_{xb} &= k_{xb} + jwd_{xb} \\ A_{ya} &= k_{ya} + jwd_{ya} \\ A_{yb} &= k_{yb} + jwd_{yb} \end{aligned} \quad (5)$$

Eq.(4) is rebuilt by substitution of Eq.(5). It can be written as

$$\begin{bmatrix} -mw^2\frac{l_b}{l}+A_{xa} & -mw^2\frac{l_a}{l}+A_{xb} & 0 & 0 \\ -J\frac{w^2}{l}+A_{xa}l_a & J\frac{w^2}{l}-A_{xb}l_b & 0 & 0 \\ 0 & 0 & -mw^2\frac{l_b}{l}+A & -mw^2\frac{l_a}{l}+A_{yb} \\ 0 & 0 & -J\frac{w^2}{l}+A_{ya}l_a & J\frac{w^2}{l}-A_{yb}l_b \end{bmatrix} \quad (6)$$

$$\begin{bmatrix} x_a(jw) \\ x_b(jw) \\ y_a(jw) \\ y_b(jw) \end{bmatrix} = \begin{bmatrix} F_x(jw) \\ M_x(jw) \\ F_y(jw) \\ M_y(jw) \end{bmatrix}$$

Obviously, Eq.(6) is the linear equations of complex number with four unknowns, which are $A_{xa}, A_{xb}, A_{ya}, A_{yb}$. In the parameter identification, $[F_x(jw), M_x(jw), F_y(jw), M_y(jw)]^T$ are the excitation signals and $[x_a(jw), x_b(jw), y_a(jw), y_b(jw)]^T$ are the displacement responses. They all are known quantities. Therefore, $A_{xa}, A_{xb}, A_{ya}, A_{yb}$ can be solved as follows

$$A_{xa} = \frac{F_x(jw)l_b + M_x(jw) + \left(mw^2\frac{l_al_b}{l} - J\frac{w^2}{l}\right)x_b(jw)}{x_a(jw)l} + mw^2\frac{l_b^2}{l^2} + J\frac{w^2}{l^2}$$

$$A_{xb} = \frac{F_x(jw)l_a - M_x(jw) + \left(mw^2\frac{l_al_b}{l} - J\frac{w^2}{l}\right)x_a(jw)}{x_b(jw)l} + mw^2\frac{l_a^2}{l^2} + J\frac{w^2}{l^2}$$

$$A_{ya} = \frac{F_y(jw)l_b + M_y(jw) + \left(mw^2\frac{l_al_b}{l} - J\frac{w^2}{l}\right)y_b(jw)}{y_a(jw)l} + mw^2\frac{l_b^2}{l^2} + J\frac{w^2}{l^2}$$

$$A_{yb} = \frac{F_y(jw)l_a - M_y(jw) + \left(mw^2\frac{l_al_b}{l} - J\frac{w^2}{l}\right)y_a(jw)}{y_b(jw)l} + mw^2\frac{l_a^2}{l^2} + J\frac{w^2}{l^2}$$

(7)

Finally, the equivalent stiffness and equivalent damping can be deduced as

$$\begin{aligned} k_{xa} &= \mathrm{Re}\{A_{xa}\} & ; & \quad d_{xa} &= \mathrm{Im}\{A_{xa}\}/w \\ k_{xb} &= \mathrm{Re}\{A_{xb}\} & ; & \quad d_{xb} &= \mathrm{Im}\{A_{xb}\}/w \\ k_{ya} &= \mathrm{Re}\{A_{ya}\} & ; & \quad d_{ya} &= \mathrm{Im}\{A_{ya}\}/w \\ k_{yb} &= \mathrm{Re}\{A_{yb}\} & ; & \quad d_{yb} &= \mathrm{Im}\{A_{yb}\}/w \end{aligned} \quad (8)$$

Where, $\mathrm{Re}\{\ \}$ and $\mathrm{Im}\{\ \}$ respectively is to obtain the real part and imaginary part of a complex number.

4. Schroeder Phased Harmonic Sequences

The multi-frequency excitation is the normal method for parameter identification of AMB. For the AMB system, however, if all the frequency components of multi-frequency excitation are arbitrarily added together, the resulting response may produce unacceptably large rotor vibration or cause force saturating of the magnetic bearing, which may sharply increase the undesired nonlinearity of measurement. It is not a good solution to decrease the excitation amplitude of every frequency, because this will result in weak perturbation in the frequency domain and consequently increase the identification errors.

Schroeder Phased Harmonic Sequences(SPHS)[11] can achieve the lowest possible peak value signal by means of superimposing these components with appropriate selection of the relative phasing, so that the possibility of the vibration displacement exceeding clearance or the bearing force reaching saturation is minimized.

4.1 Composing of SPHS

SPHS reduces the peak value by re-organizing the relative phasing of each harmonic. The Composing of SPHS is very simple and its expression is given by

$$x(t) = \sum_{k=1}^{N}\sqrt{2P_k}\cos(2kpt/T + q_k) \quad (9)$$

Where, N is the number of harmonics, T is the period of the fundamental-harmonic, P_k is the power of the kth harmonic.(if signal is $A\cos(2pt/T)$, its power is $A^2/2$, so $\sqrt{2P_k}$ is the amplitude of the kth harmonic, q_k is the phase angle of the kth harmonic.)

In order to obtain the lowest peak value of harmonics superimposing, SPHS designates the phase angle of each harmonic as follows

$$q_k = q_1 - 2p\sum_{i=1}^{k-1}(k-i)P_i \qquad (10)$$

Where, q_1 is the phase angle of the fundamental-harmonic, which can be assigned at will. In most applications of SPHS, q_1 will be assigned as 0 or p. Then, Eq.(10) can be modified as

$$q_k = p[[\sum_{i=1}^{k-1}(k-i)P_i]] \qquad (11)$$

Where, $[[\ ]]$ computes the largest integer not larger than their contents, namely, rounding operation.

Eq.(11) can be further simplified if all of harmonics have the same amplitude, namely, it!s the flat-spectrum signal, $P_i = P/N(i=1,2,\cdots,N)$, then

$$q_k = p[[k^2/2N]] \qquad (12)$$

Eq(12) is the most simplified SPHS representation, which is widely used in practical applications.

4.2 Illustrative Examples of SPHS

In this section, the illustrative examples comparing the SPHS signal with the non-SPHS signal will be given.

Let the frequency of the fundamental harmonic is 1Hz, the amplitude of all harmonics are 1 unit, the number of harmonics are respectively given as N=25 50 100. For the non-SPHS signal, the phase angles of all harmonics are always defined as $q_i = 0$ $(i=1,2,\cdots,N)$, which is called zero phase angle signal in this paper. The illustrative examples for comparing are shown from Fig.2 to Fig.7.

It can be observed that the peak value of the zero phase angle signal sharply increases with the harmonics number growing. The peak value are about 20,40,80 for N=25 50 100 respectively. Contrastively, the peak value of SPHS increases gently in spite of the number of harmonics being doubled and redoubled. The peak value are about 9,12,15 for N=25 50 100 respectively. By all appearances, if the zero phase angle signal is adopted, the possibility of the vibrationt exceeding clearance or the magnetic force reaching saturation will be greater.

Fig.2 N=25 zero phase angle signal   Fig.3 N=50 zero phase angle signal   Fig.3 N=100 zero phase angle signal
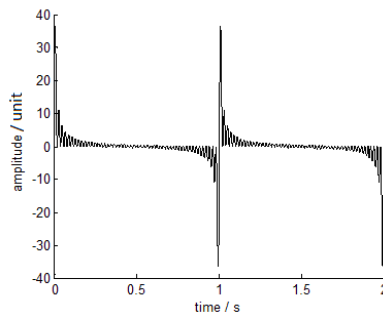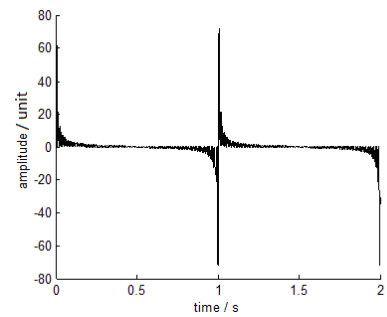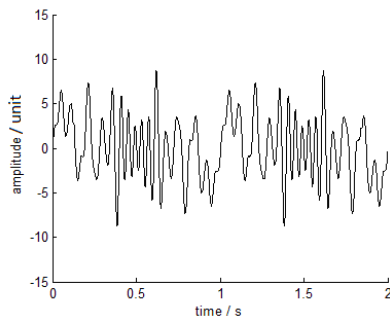

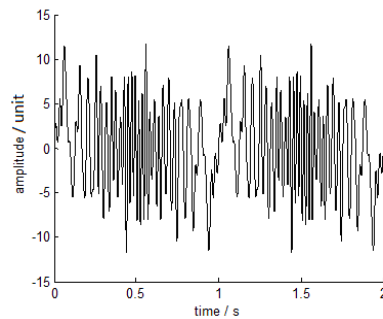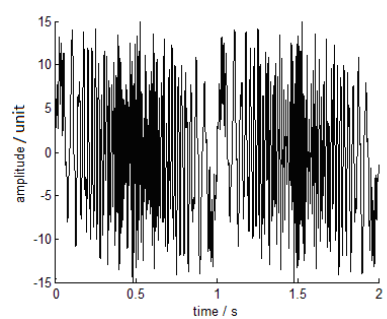Fig.5 N=25   SPHS signal   Fig.6 N=50   SPHS signal   Fig.7 N=100   SPHS signal

5.   Experiment

5.1 AMB Rig

To evaluate the effectiveness of the proposed method, The experiments were carried out on a rig of

AMB flywheel rotor system with vertical shaft structure as shown in Fig. 8. The axial support for the rotor is provided by a permanent magnetic bearing and the radial support by two radial AMBs, upper AMB and lower AMB. The equivalent stiffness and the equivalent

damping of two radial AMBs need measuring in expectation. Fig.9 is the drawing of rotor structure, whose parameters are that the rotor mass including flywheel is m=58.32kg, the transverse moment of inertia is J=1.878 $\mathrm{kg} \times \mathrm{m}^2$, the clearance of touch-down bearing is 0.2mm, $l_a = 305\mathrm{mm}$, $l_b = 222\mathrm{mm}$. The force-current factor of the upper AMB is 326N/A, and that of the lower is 111.32N/A. The experiments were operated on the d-SPACE DS1103 with the decentralized PID control for rotor levitating.

Firstly, for checking the vibration condition, the amplitude-frequency characteristics of the rotor vibration are carefully measured. When the excitation is imposed on the upper AMB, the amplitude-frequency characteristics of 4 directions in two radial AMB are shown in Fig.10 and Fig.11. It can be observed that there are some peaks of rotor vibration in the range of 20Hz-60Hz. Among them, the vibration peaks in 26Hz and 54Hz are the two highest peaks, which may be, by

estimate, the critical frequency(resonance frequency) of cylindrical mode and conical mode of rotor motion. Because the critical frequency values of every directions are different and close each other, so that their vibration peaks are close one another and crowd in the range of 20Hz-60Hz. When the frequency is beyond 80Hz, the amplitude-frequency characteristic sharply descends close to zero.

Fig.8 rig of AMB flywheel rotor system
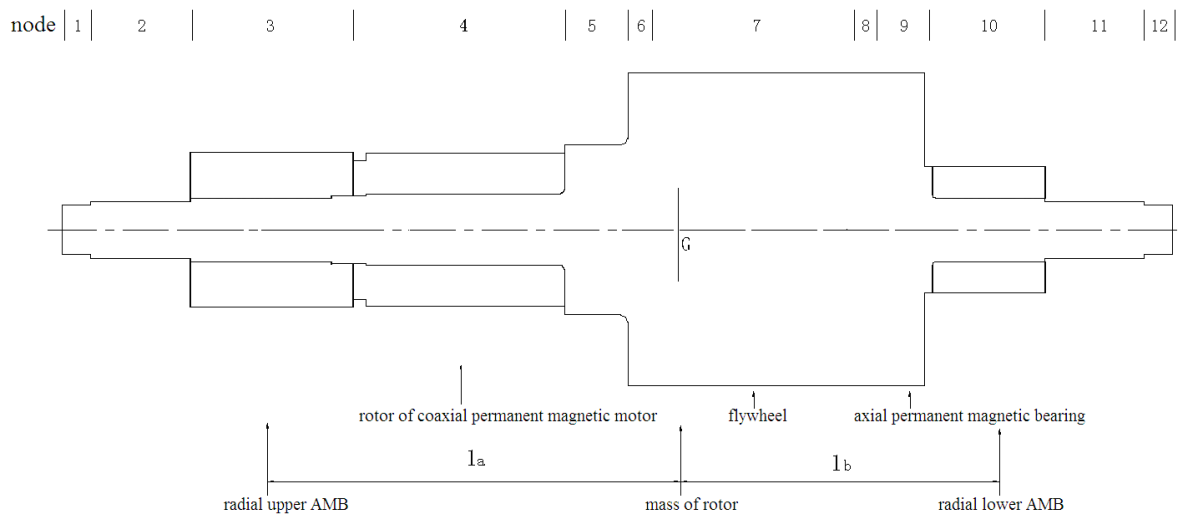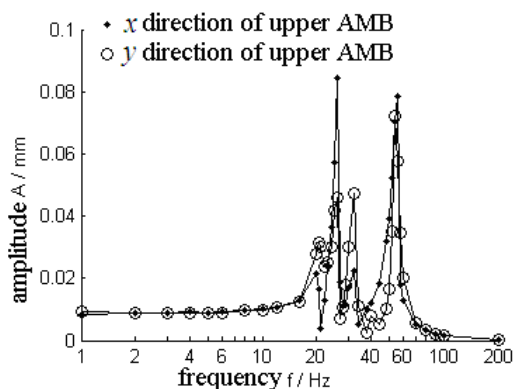

Fig.9 rotor structure drawing

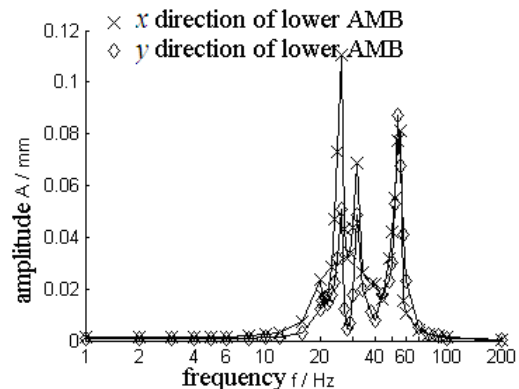Fig.10 amplitude -frequency characteristic of upper AMB

Fig.11 amplitude -frequency characteristic of lower AMB

5.2 Test for SPHS Effectiveness

In this test, the contrasts of the practical effectiveness between SPHS and zero phase angle signal will be tested in expectation.

A rotating vector-like signal is injected into the control current of the upper AMB, that is, all the sine harmonics are injected into x direction and all the cosine harmonics are injected into y direction. Therefore, the magnetic exciting force in every harmonics frequency are all the rotating vector. The adopted multi-frequency excitation is a flat-spectrum signal in the range of 1-200Hz. The fundamental-harmonic is 1Hz and N=200. In test, the amplitudes of harmonics are respectively set up as 0.4N, 0.8N, 1.2N, 1.6N.
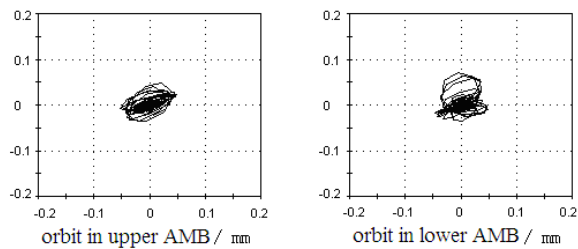
The experiments will record the practical rotor vibration orbit under the different amplitude of excitation. Fig.12 and Fig.13 are the response orbit for the excitation harmonics amplitude of 0.4N. Fig.14 and Fig.15 are that of 0.8N. It is clearly that the greater the excitation harmonic amplitude is, the more the vibration response orbit enlarges. However, the rotor orbit enlarging of zero phase angle signal is much more than that of SPHS.

It can be observed in Fig.14 that, when the excitation amplitude reaches to 0.8N for zero phase angle signal, the rotor orbit in lower AMB is close 0.2mm and it meams that the rotor just comes into contact with the touch down bearing. It implies that the excitation amplitude can not be increased any more in the case of zero phase angle signal.

Fig.12 response orbit of 0.4N with zero phase angle

Fig.13 response orbit of 0.4N with SPHS

Fig.14 response orbit of 0.8N with zero phase angle
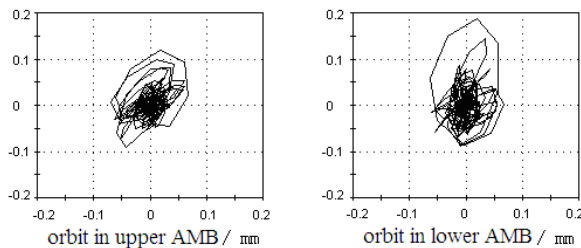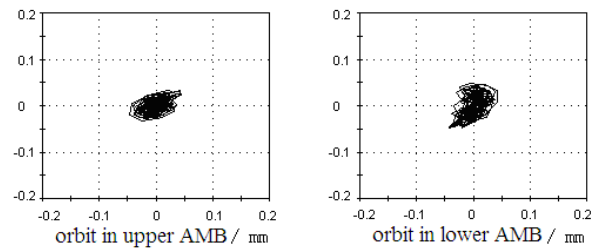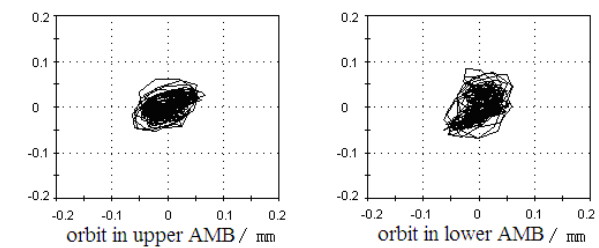

Fig.15 response orbit of 0.8N with SPHS

Then, the excitation amplitude continues to be increased for SPHS. Fig.16 is the rotor orbit for the excitation amplitude increasing to 1.2N with SPHS and Fig.17 is for 1.6N. The vibration orbit enlarges with the excitation increasing. For SPHS, when the excitation amplitude reaches to 1.7N, the rotor evidently contacts the touch down bearing.

It is concluded that, the upper limit of excitation harmonics amplitude is 1.6N for SPHS, and 0.8N for the zero phase angle signal. It proves that SPHS can efficiently minimize the peak value for the superimposed multi-frequency signal.
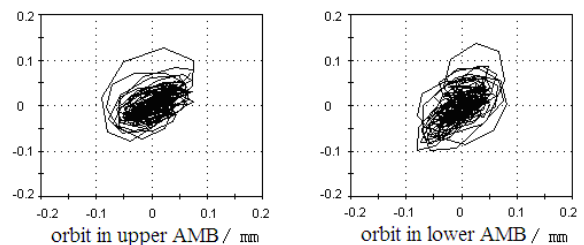

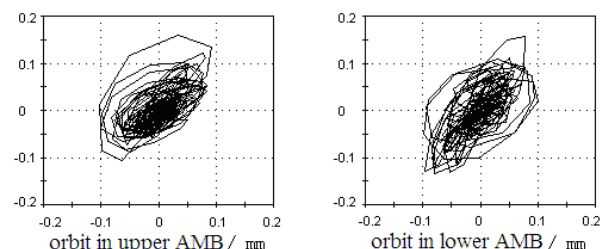
Fig.16 response orbit of 1.2N with SPHS

Fig.17 response orbit of 1.6N with SPHS

5.3 Measuring Stiffness and Damping with multi-frequency excitation

According to Eq.(7)and (8), the equivalent stiffness and the equivalent damping in 4 directions of the AMB rig will be measured by the proposed method.

Fig.18 is the measurement results of the equivalent stiffness under the excitation harmonics amplitude of 1.6N. Because the equivalent stiffness in 4 directions is similar to each other, the corresponding direction of each diagram line for the equivalent stiffness is not denoted in Fig.18. The equivalent stiffness of AMB increases gradually along with the frequency rising, which is the same conclusion drawn in other academic literatures[5,9,10].

Fig.18 shows that the measuring values have a visible drop in the band of critical frequency (resonance frequency) in the range of 20Hz-60Hz. The reason is that the rotor vibration is much great in the band of critical frequency. The greater the rotor vibration displacement is, the larger control current is needed. The AMB of the experiment rig adopts the differential mechanism. When the control current is less than the bias current, the magnetic force would be twice produced by both two sides AMB poles. Correspondingly, when the control current is more than the bias current, the magnetic force would only be produced by one pole of single side in the AMB. Consequently, the equivalent stiffness would drop, when the control current is more than the bias current. The same phenomenon have been observed in the reference[10].

Above 80Hz, the diagram lines of the equivalent stiffness is in disorder for identification errors due to the rotor weak vibrating.

The measurement results of the equivalent damping are shown in Fig.19 with the excitation harmonics amplitude of 1.6N. It is visible that the equivalent damping values are very little in most frequency, and also is disordered for identification errors beyond 80Hz.
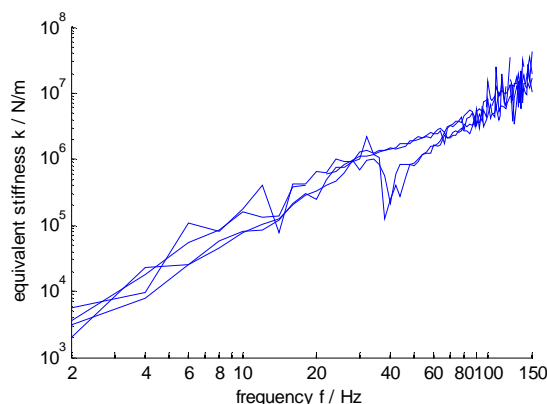

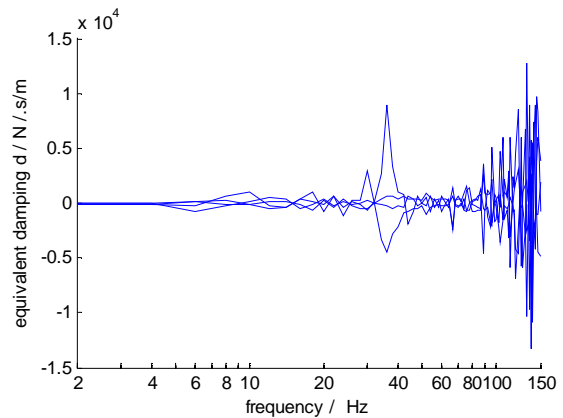Fig.18 equivalent stiffness in 4 directions under 1.6N excitation

Fig.19 equivalent damping in 4 directions under 1.6N excitation

6. Conclusion

In this study, a method for measuring the equivalent stiffness and the equivalent damping is proposed based on the multi-DOF rotor model. SPHS is adopted in the multi-frequency excitation to achieve the lowest possible peak value signal by means of appropriate selection for the relative phasing of each component without decreasing the amplitude of every components, so that the possibility of the vibration displacement exceeding clearances or the bearing force reaching saturation is minimized.

Finally, the experiments indicate that the proposed method can correctly identify the equivalent stiffness and the equivalent damping of the AMB-rotor system. It really has the better practical utility for the dynamic analysis of AMB.

Acknowledgement

References

[1] N. Tsai, H. Li, C. Lin, et al. Identification of rod dynamics under influence of active magnetic bearing[J]. Mechatronics. 2011, 21(4): 1013-1024.

[2] T. Lim and S. Cheng. Parameter estimation and statistical analysis on frequency dependent active control forces[J]. Mechanical Systems and Signal Processing. 2007, 21(5):2112-2124.

[3] S. Kim and C. Lee. On-line identification of current and position stiffness by LMS algorithm in active magnetic bearing system

equipped with force transducers[J]. Mechanical Systems and Signal Processing. 1999, 13(5): 681-690.

[4] N. Mehmet, O. Matthew, T. Cole, et al. On the use of Schroeder phased harmonic sequences in multi-frequency vibration control of flexible rotor/magnetic bearing systems[C]. Proceedings of 8th International Symposium on Magnetic Bearings. Mito, Japan, 2002, pp:218-222.

[5] T. Lim, S. Cheng and C. Poh. Parameter estimation of one-axis magnetically suspended system with a digital PID controller[C]. Proceedings of 1st International Conference on Sensing Technology. New Zealand, 2005, pp:419-424.

[6] H. Bauomy. Stability analysis of a rotor-AMB system with time varying stiffness[J]. Journal of the Franklin Institute. 2012, 349(2): 1871 1890.

[7] F. Sayyad and N. Gadhave. Variable stiffness type magnetic vibration absorber to control the vibration of beam structure[J]. Journal of Vibration and Control. 2013, 7, published online:1-7.

[8] M. Baloh, G. Tao and P. Allaire. Adaptive estimation of magnetic bearing parameters[C]. Proceedings of the IEEE International Conference on Control Applications. Hawaii, USA, 1999, pp:1193-1198.

[9] Yang Zuoxing, Zhao Lei, Zhao Hongbi. Automatic measurement of dynamic stiffness for active magnetic bearings[J]. Chinese Journal of Mechanical Engineering. 2001, 37(3):25-29. (in Chinese)

[10] Jiang Kejian, Zhu Changsheng. On-line Measurement of Supporting Characteristics of an Active Magnetic Levitations with Unknown Transfer Function[J]. China Mechanical Engineering. 2010, 21(8): 883-888. (in Chinese)

[11] M. Schroeder. Synthesis of Low-Peak-Factor Signals and Binary Sequences with Low Autocorrelation [J]. IEEE Transaction on Information Theory. 1970, 16(1): 85-89.